

Verification of non-equal-time commutators of a trapped ion

F. Krumm* and W. Vogel

Arbeitsgruppe Theoretische Quantenoptik, Institut für Physik, Universität Rostock, D-18059 Rostock, Germany

(Dated: July 8, 2022)

The vibronic dynamics of a trapped ion can be described by the explicitly time-dependent nonlinear Jaynes-Cummings model. It is shown that the expectation value of the interaction Hamiltonian and its non-equal-time commutator can be determined by measuring the electronic-state evolution. This yields direct insight in the time-ordering contributions to the unitary time evolution. Data simulations show that this information can be extracted from measured quantities.

INTRODUCTION

Starting with the development of quantum mechanics and the introduction of Hilbert-space operators, the non-commutativity of the latter became an issue. It leads to many fascinating physical effects, where the most prominent example is most likely the Heisenberg uncertainty principle [1–3]. Furthermore, non-commutativity plays an important role in quantum field theory [4], quantum many-body systems [5–13], quantum electrodynamics [14–16], the standard model [17], and cosmology [18, 19]. Here we consider the problem of non-equal-time commutators from the quantum optics point of view.

A noteworthy achievement in this context is the experimental verification of the bosonic commutation relation, $[\hat{a}, \hat{a}^\dagger] = \hat{1}$. Although this relation is of fundamental relevance for the formulation of quantum mechanics, it was not verified before 2007, in a seminal paper by Bellini and co-authors [20]. Later on, this subject was analyzed in some more detail [21, 22]. Elementary commutation rules of such a type are equal-time rules introduced in the procedure of canonical quantization.

This leads to another fundamental subject, namely the non-equal-time commutation rules, which play an important role in the context of interaction problems including *time ordering*. If the dynamics of an explicitly time-dependent Hamiltonian is formally solved in terms of the standard time-evolution operator, one finds that the latter obeys a time-ordering prescription, cf., e.g., [23–26]. This prescription must not be omitted as it has crucial impact on the dynamics of the system [27–34]. Paradoxically, despite its key role in basic quantum mechanics, detailed treatments of time-ordering effects are rarely available. A direct verification of non-equal-time commutators of Hamiltonians has, to our best knowledge, not been studied yet.

In the present paper, we use basic relations of quantum mechanics to show that the measurement of the expectation value of an explicitly time-dependent interaction Hamiltonian yields the expectation value of a partly integrated non-equal-time commutator of this Hamiltonian. If this commutator is non-zero, the system undergoes a time-ordered dynamics. In principle, the lat-

ter can be verified for any physical system with a time-dependent Hamiltonian, which is a keystone of quantum theory. Here, we examine the off-resonantly driven nonlinear Jaynes-Cummings model, which describes the vibronic dynamics of a trapped ion. The advantage of this model is that we may obtain the expectation value of the interaction Hamiltonian directly from the measurement of the excited electronic-state occupation probability. The details of the procedure will be demonstrated by the use of simulated data.

TIME EVOLUTION

We start with some fundamental relations of quantum theory. The properties of a physical system may be compactly expressed by its Hamiltonian, $\hat{H}_S(t) = \hat{H}_{0,S} + \hat{H}_{\text{int},S}$. The index S denotes the Schrödinger picture, $\hat{H}_{0,S}$ is the free evolution of the system, and $\hat{H}_{\text{int},S}$ is the interaction of different degrees of freedom. In the interaction picture, denoted by the index I , and assuming that the interaction Hamiltonian is in this picture explicitly time-dependent, the dynamics of the system is described by the time-evolution operator

$$\hat{U}_I(t) = \mathcal{T} \exp \left(-\frac{i}{\hbar} \int_0^t \hat{H}_{\text{int},I}(\tau) d\tau \right). \quad (1)$$

Here, \mathcal{T} denotes the time-ordering prescription which only can be ignored if the interaction Hamiltonian commutes with itself at different times, $[\hat{H}_{\text{int},I}(\tau_1), \hat{H}_{\text{int},I}(\tau_2)] = 0$, $\forall(\tau_1, \tau_2)$, see for example [23–26]. We emphasize that throughout this work the time dependence of the Hamiltonian $\hat{H}_{\text{int},I}(\tau)$ refers to the explicit time dependence and not to the (implicit) time dependence of the operators. The latter is directly caused by the time-evolution operator $\hat{U}_I(t)$. In general, the interaction Hamiltonian is proportional to some coupling constant $|\kappa|$ and, hence, we may use a power series expansion

$$\begin{aligned} \hat{U}_I(t) = & 1 - \frac{i}{\hbar} \int_0^t d\tau_1 \hat{H}_{\text{int},I}(\tau_1) \\ & - \frac{1}{\hbar^2} \int_0^t d\tau_1 \int_0^{\tau_1} d\tau_2 \hat{H}_{\text{int},I}(\tau_1) \hat{H}_{\text{int},I}(\tau_2) + \mathcal{O}(|\kappa|^3). \end{aligned} \quad (2)$$

The full time evolution of the interaction Hamiltonian reads as,

$$\begin{aligned} \hat{U}_I^\dagger(t) \hat{H}_{\text{int},I}(t) \hat{U}_I(t) \\ = \underbrace{\hat{H}_{\text{int},I}(t)}_{\propto |\kappa|} + \frac{i}{\hbar} \int_0^t d\tau_1 \underbrace{\left[\hat{H}_{\text{int},I}(\tau_1), \hat{H}_{\text{int},I}(t) \right]}_{\propto |\kappa|^2} + \mathcal{O}(|\kappa|^3). \end{aligned} \quad (3)$$

The terms proportional to $|\kappa|$ and $|\kappa|^2$ yield the interaction Hamiltonian and its partly integrated non-equal-time commutator, respectively. Let us apply this result to a realistic model—the explicitly time-dependent nonlinear Jaynes-Cummings Hamiltonian, which describes the vibronic dynamics of a trapped ion.

NONLINEAR JAYNES-CUMMINGS MODEL

The quantized center-of-mass motion of a trapped ion, in the resolved sideband limit, can be described by the nonlinear Jaynes-Cummings model [35]. Including a frequency mismatch, such that the Hamiltonian is explicitly time-dependent in the interaction picture, the corresponding interaction Hamiltonian reads [36]

$$\hat{H}_{\text{int},I}(t) = \hbar|\kappa|e^{-i\Delta\omega t+i\theta} \hat{A}_{21} \hat{f}_k(\hat{n};\eta) \hat{a}^k + \text{H.c.} \quad (4)$$

Here, $\kappa = |\kappa|e^{i\theta}$ is the coupling constant of the ion's electronic and vibrational levels and is proportional to the amplitude of the driving laser. Additionally, \hat{a} and \hat{a}^\dagger are the annihilation and creation operators of the vibrational mode and, in the case of a standing wave, with $\hat{n} = \hat{a}^\dagger \hat{a}$, $\hat{f}_k(\hat{n};\eta)$ describes the mode structure of the driving laser field at the position of the ion. It is, in Fock basis, defined as follows:

$$\begin{aligned} \hat{f}_k(\hat{n};\eta) \\ = \frac{1}{2} e^{i\Delta\phi - \eta^2/2} \sum_{n=0}^{\infty} |n\rangle \langle n| \frac{(i\eta)^k n!}{(n+k)!} L_n^{(k)}(\eta^2) + \text{H.c.}, \end{aligned} \quad (5)$$

with $L_n^{(k)}$ denoting the generalized Laguerre polynomials, η is the Lamb-Dicke parameter, and $\Delta\phi$ determines the position of the trap potential relative to the laser wave. The atomic flip operator $\hat{A}_{ij} = |i\rangle \langle j|$ ($i, j = 1, 2$) describes the $|j\rangle \rightarrow |i\rangle$ transition. Furthermore, the classical driving-laser with frequency $\omega_L = \omega_{21} - k\nu + \Delta\omega$ is slightly detuned from the k -th sideband by $\Delta\omega$, which yields the time-dependence of the Hamiltonian in Eq. (4). Here, ν is the trap frequency and $\omega_{21} = \omega_2 - \omega_1$ is the separation of the electronic levels $|1\rangle$ and $|2\rangle$. Finally, the Hamiltonian describing the free evolution reads as

$$\hat{H}_{0,I} = \hbar\nu\hat{n} + \hbar\omega_{21}\hat{A}_{22}. \quad (6)$$

A detailed discussion of the Hamiltonians can be found in Refs. [35, 36] or Chap. 13 of [24].

The solution of the corresponding dynamics,

$$\begin{aligned} \hat{U}_I(t) = \sum_{n=0}^{\infty} \left(a_n(t) |2, n\rangle \langle 2, n| \right. \\ \left. - b_n^*(t) e^{-2i\theta} |1, n+k\rangle \langle 2, n| + b_n(t) e^{2i\theta} |2, n\rangle \langle 1, n+k| \right. \\ \left. + a_n^*(t) |1, n+k\rangle \langle 1, n+k| \right) + \sum_{q=0}^{k-1} |1, q\rangle \langle 1, q|, \end{aligned} \quad (7)$$

with

$$a_n(t) = e^{-i\Delta\omega t/2} \left[\cos(\Gamma_n t) + \frac{i\Delta\omega}{2\Gamma_n} \sin(\Gamma_n t) \right], \quad (8)$$

$$b_n(t) = e^{-i\Delta\omega t/2} \frac{|\kappa|w_n}{i\Gamma_n} \sin(\Gamma_n t),$$

$$\Gamma_n = \sqrt{\left(\frac{\Delta\omega}{2} \right)^2 + w_n^2 |\kappa|^2},$$

$$w_n = \cos\left(\Delta\phi + \frac{\pi}{2}k\right) \eta^k e^{-\eta^2/2} \sqrt{\frac{n!}{(n+k)!}} L_n^{(k)}(\eta^2)$$

has been derived in Ref. [37].

Let us consider the time evolution of the occupation probability of the excited electronic state, $\sigma_{22} = \langle \hat{A}_{22} \rangle$. Because of $[\hat{A}_{22}, \hat{H}_{0,I}] = 0$, σ_{22} depends solely on the interaction Hamiltonian, which yields

$$\dot{\sigma}_{22}(t) = \frac{i}{\hbar} \left\langle \hat{U}_I^\dagger(t) \left[\hat{H}_{\text{int},I}(t), \hat{A}_{22} \right] \hat{U}_I(t) \right\rangle. \quad (9)$$

Using the Hamiltonian in Eq. (4), we obtain

$$\begin{aligned} \dot{\sigma}_{22}(t) = i|\kappa| \left\langle -e^{-i\Delta\omega t+i\theta} \hat{A}_{21}(t) \hat{f}_k(\hat{n}(t);\eta) \hat{a}^k(t) \right. \\ \left. + e^{i\Delta\omega t-i\theta} \hat{A}_{12}(t) \hat{a}^{\dagger k}(t) \hat{f}_k(\hat{n}(t);\eta) \right\rangle. \end{aligned} \quad (10)$$

Comparing this expression with the Hamiltonian (4), for $\Delta\omega \neq 0$ we get

$$\dot{\sigma}_{22}(t) \equiv \frac{1}{\hbar\Delta\omega} \left\langle \hat{U}_I^\dagger(t) \left(\frac{d}{dt} \hat{H}_{\text{int},I}(t) \right) \hat{U}_I(t) \right\rangle. \quad (11)$$

Since $\hat{U}_I^\dagger(t) \frac{d}{dt} \hat{H}_{\text{int},I}(t) \hat{U}_I(t) = \frac{d}{dt} \left(\hat{U}_I^\dagger(t) \hat{H}_{\text{int},I}(t) \hat{U}_I(t) \right)$, we may integrate Eq. (10) to arrive at

$$\begin{aligned} \sigma_{22}(t) - \sigma_{22}(0) = \frac{1}{\hbar\Delta\omega} \left(\left\langle \hat{U}_I^\dagger(t) \hat{H}_{\text{int},I}(t) \hat{U}_I(t) \right\rangle \right. \\ \left. - \left\langle \hat{U}_I^\dagger(0) \hat{H}_{\text{int},I}(0) \hat{U}_I(0) \right\rangle \right). \end{aligned} \quad (12)$$

Thus, the measurement of the excited-state occupation probability $\sigma_{22}(t)$, which is achieved via probing an auxiliary transition for resonance fluorescence [38–40], is directly related to the expectation value of the time-dependent interaction Hamiltonian. The consideration of different orders with respect to $|\kappa|$ allows one to determine either the interaction Hamiltonian itself or the corresponding commutator in Eq. (3). Without loss of generality, we set $\theta = 0$ in the following.

DETERMINATION OF THE INTERACTION HAMILTONIAN

Let us consider the determination of the interaction Hamiltonian in Fock basis, $\text{Tr}_{\text{el}}(\hat{\sigma}(0)\langle n|\hat{H}_{\text{int},I}(t)|n\rangle)$, for $k = 0$ in Eq. (4). Here, Tr_{el} is the trace over the electronic degrees of freedom. The generation of vibrational Fock states in an ion trap was already investigated in the 1990s, cf. Refs. [41, 42]. In the following we use the input density matrix $\hat{\rho}(0) = \hat{\sigma}(0) \otimes \hat{\rho}_{\text{mot}}(0)$, where $\hat{\sigma}(0)$ and $\hat{\rho}_{\text{mot}}(0)$ describe the electronic and the motional input state, respectively. If the electronic state is initially in a superposition,

$$\hat{\sigma}(0) = (\gamma_1|1\rangle + \gamma_2|2\rangle)(\gamma_1^*\langle 1| + \gamma_2^*\langle 2|), \quad (13)$$

with $|\gamma_1|^2 + |\gamma_2|^2 = 1$, and $\hat{\rho}_{\text{mot}} = |n\rangle\langle n|$, one readily derives

$$\langle \hat{U}_I^\dagger(0)\hat{H}_{\text{int},I}(0)\hat{U}_I(0) \rangle = \hbar|\kappa|f_0(n;\eta)(\gamma_1\gamma_2^* + \gamma_2\gamma_1^*). \quad (14)$$

Here we defined $f_k(n;\eta) = \langle n|\hat{f}_k(\hat{n};\eta)|n\rangle$. Hence, if $\arg(\gamma_1) - \arg(\gamma_2) = (2m+1)\frac{\pi}{2}$ for $m = 0, 1, \dots$, then the expectation value in Eq. (14) becomes zero. Thus, we set $\gamma_1 = e^{i\pi/2}/\sqrt{2}$ and $\gamma_2 = 1/\sqrt{2}$, which leads to $\sigma_{22}(0) = 1/2$. Hence, Eq. (12) simplifies to

$$\langle \hat{U}_I^\dagger(t)\hat{H}_{\text{int},I}(t)\hat{U}_I(t) \rangle = \hbar\Delta\omega(\sigma_{22}(t) - 1/2). \quad (15)$$

To demonstrate the applicability, we simulate the scenario using random events for the evolution of $\sigma_{22}(t)$. For convenience, we introduce the dimensionless coupling g via $|\kappa| \rightarrow g|\kappa'|$ and the dimensionless time $|\kappa'|t$. A first result of the basic procedure is shown in Fig. 1 for a fixed time. Therein, each value of σ_{22} (blue dots) is obtained from 10^3 random events. They are fitted by the polynomial

$$\tilde{\sigma}_{22} - \frac{1}{2} = \sum_{n \geq 0} c_{2n+1}g^{2n+1}. \quad (16)$$

In the fit function only odd orders of g appear, due to the structure of the Hamiltonian (4) and our choice of the electronic input state. The parameter c_1 leads to the desired Hamiltonian, cf. Eq. (3), and is visualized in Fig. 1 via the dashed red line. It is obvious that especially at $g \ll 1$ a meticulous resolution of the data is important.

Repeating this procedure for various Fock input states yields the interaction Hamiltonian in Fock-space representation, see Fig. 2. Here we increased the number of random events to 5×10^3 . The theoretical prediction (gray bars) is easily calculated to be

$$\langle \hat{H}_{\text{int},I}(t) \rangle = \hbar|\kappa|f_0(n;\eta)(\gamma_1\gamma_2^*e^{-i\Delta\omega t} + \gamma_2\gamma_1^*e^{i\Delta\omega t}). \quad (17)$$

The results of the simulation are close to the analytical results, they can be further improved by increasing the number of random events.

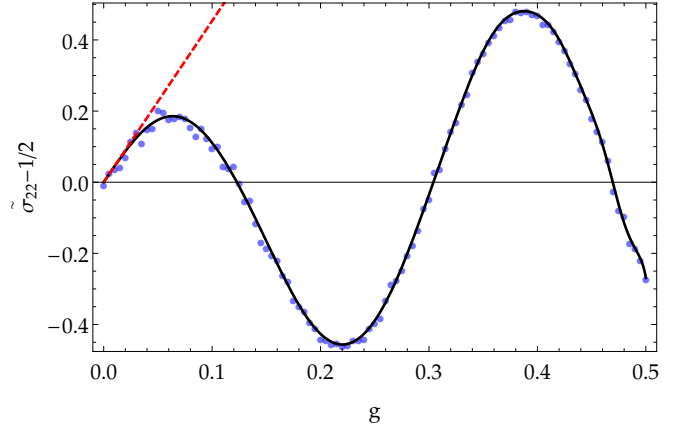


FIG. 1. The simulated data (blue dots) of the excited state occupation probability together with a nonlinear curve fit [Eq. (16)] for the excitation to the zeroth sideband, $k = 0$, at $|\kappa'|t = 10$ (solid black line). The motional input state is the ground state $|0\rangle$. The quantity $c_1 g$ is given as the dashed red line. Parameters: $\eta = 0.2$, $\Delta\omega/|\kappa'| = 0.2$, $\Delta\Phi = 0$, and $\nu = 5000$.

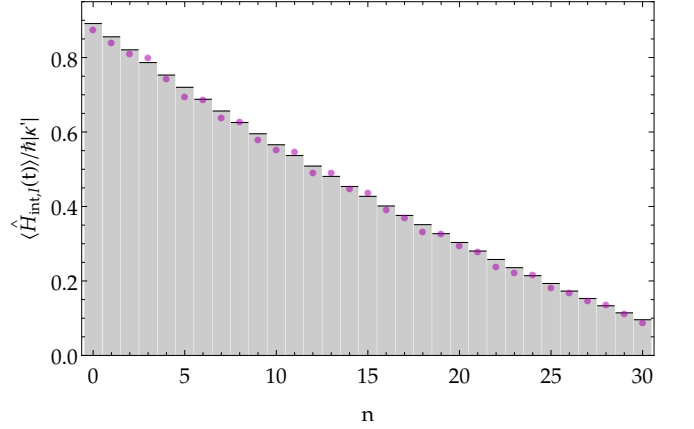


FIG. 2. Simulated data (magenta dots) obtained by the technique in Fig. 1, for motional Fock-states $|n\rangle$ at $|\kappa'|t = 10$. The other parameters are the same as in Fig. 1. The gray bars represent the analytical results in Eq. (17).

VERIFICATION OF THE COMMUTATOR

For this task we use $\hat{\sigma}(0) = |1\rangle\langle 1|$. Hence, the ion is initially in the electronic ground state, so that $\sigma_{22}(0) = 0$. From Eq. (12) we get

$$\langle \hat{U}_I^\dagger(t)\hat{H}_{\text{int},I}(t)\hat{U}_I(t) \rangle = \hbar\Delta\omega\sigma_{22}(t). \quad (18)$$

Furthermore, we assume that the vibrational input state is a coherent state $|\alpha_0\rangle$. Details concerning the preparation of coherent motional states can be found for example in Ref. [41].

In Fig. 3 we outline the basic procedure, where the statistics is simulated with 10^4 random events for each data point. The simulated data are now fitted by the

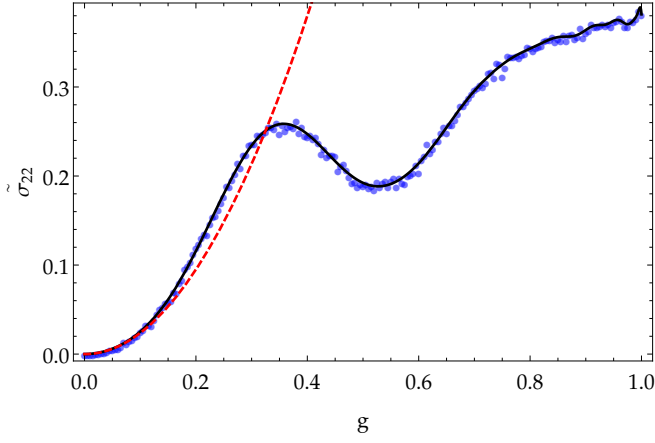


FIG. 3. The simulated data (blue dots) of the excited state occupation probability together with a nonlinear curve fit $\tilde{\sigma}_{22}$ [Eq. (19)] for the excitation to the second sideband, $k = 2$, are shown for $|\kappa'|t = 40$ (solid black line). The quantity $c_2 g^2$ is given as the dashed red line. Parameters: $\alpha_0 = \sqrt{12}$, $\eta = 0.2$, $\Delta\omega/|\kappa'| = 0.2$, $\Delta\Phi = 0$, and $\nu = 5000$.

function

$$\tilde{\sigma}_{22} = \sum_{n \geq 1} c_{2n} g^{2n}. \quad (19)$$

For similar reasons as in Eq. (16) now only even orders of g appear. According to Eq. (3), the parameter c_2 yields the desired time-integrated commutator in Eq. (3). The parameter c_2 is visualized in Fig. 3 by the dashed red line and describes the quadratic contribution which represents the sought commutator.

To finally obtain the time-evolution of the commutator one has to repeat the measurement for all times. The corresponding simulation is depicted in Fig. 4 for 2×10^4 random events per data point and time. For each point in time we repeat the simulation as presented in Fig. 3. Afterwards we fit the data and extract the quadratic slope. The commutator of interest—i.e., the theoretical prediction—can be analytically derived and reads as

$$\begin{aligned} & \frac{i}{\hbar} \int_0^t d\tau_1 \langle 1, \alpha_0 | [\hat{H}_{\text{int},I}(\tau_1), \hat{H}_{\text{int},I}(t)] | 1, \alpha_0 \rangle \\ &= \frac{2|\kappa|^2 \hbar}{\Delta\omega} (1 - \cos \Delta\omega t) \sum_{n=0}^{\infty} |f_k(n; \eta)|^2 \frac{|\alpha_0|^{2(n+k)}}{n!} e^{-|\alpha_0|^2}, \end{aligned} \quad (20)$$

which is a harmonic oscillation in time. This result is given as the black lines in Fig. 4. The magenta and green dots correspond to the excitation to the second ($k = 2$) and the zeroth ($k = 0$) sideband, respectively. The simulated data resemble the theoretical results sufficiently well. It is noteworthy that, to certify clear experimental evidence of the relevance of non-equal-time commutators of the interaction Hamiltonian for the system dynamics, it is sufficient to demonstrate statistically significant non-zero contributions in Fig. 4. To our best knowledge, such

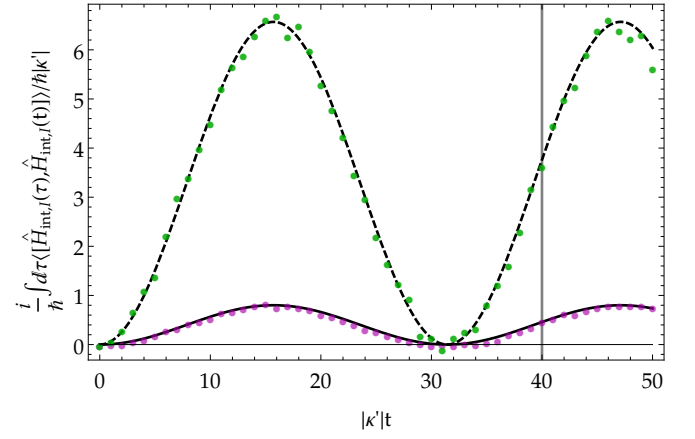


FIG. 4. The simulated data together with the theoretical predictions of the expectation value of the time-integrated commutator (black lines) from Eq. (20). The data correspond to the scenarios $k = 2$ (magenta dots) and $k = 0$ (green dots). The gray line at $|\kappa'|t = 40$ marks the situation depicted in Fig. 3 for the $k = 2$ case. The other parameters are the same as in Fig. 3.

a certification has not yet been demonstrated and it is, by the techniques proposed here, rather easy to do.

SUMMARY AND CONCLUSIONS

We have shown that, for the vibronic dynamics of a trapped ion, the measurement of the electronic-state occupation probability yields the temporal evolution of the expectation value of the interaction Hamiltonian. From this value one can both derive the expectation value of the interaction Hamiltonian in the interaction picture and the partly integrated non-equal-time commutator of the interaction Hamiltonian. The method has been applied to simulated data, for which the simulated results well approximate the analytically derived ones. This yields a powerful approach to experimentally excess the fundamentals of explicitly time-dependent temporal evolutions of quantum systems.

For the determination of the Hamiltonian we have considered an input motional Fock state and obtained the interaction Hamiltonian in Fock basis for the excitation quasi-resonant to the zeroth motional sideband. In addition, the non-equal-time commutator, which explicitly accounts for time-ordering corrections, has been investigated. For an initially prepared motional coherent state, the evolution of the time-integrated commutator has been determined. Our approach paves the way to study the explicitly time-dependent dynamics also for other quantum systems. This requires the formulation of the corresponding measurement principles for the systems of interest.

* fabian.krumm@uni-rostock.de

- [1] W. Heisenberg, Über den anschaulichen Inhalt der quantentheoretischen Kinematik und Mechanik, *Zeitschrift für Physik*, **43**, 172 (1927).
- [2] E. H. Kennard, Zur Quantenmechanik einfacher Bewegungstypen, *Zeitschrift für Physik*, **44**, 326 (1927).
- [3] P. Busch, T. Heinonen, and P. Lahti, Heisenberg's Uncertainty Principle, *Phys. Rep.* **452**, 155 (2007).
- [4] M. R. Douglas and N. A. Nekrasov, Noncommutative field theory, *Rev. Mod. Phys.* **73**, 977 (2001).
- [5] S. Khan, B. Chakraborty, and F. G. Scholtz, Role of twisted statistics in the noncommutative degenerate electron gas, *Phys. Rev. D* **78**, 025024 (2008).
- [6] C. Duval and P. A. Horvathy, The exotic Galilei group and the "Peierls substitution", *Phys. Lett. B* **479**, 284 (2000).
- [7] V. P. Nair and A. P. Polychronakos, Quantum mechanics on the noncommutative plane and sphere, *Phys. Lett. B* **505**, 267 (2001).
- [8] R. Banerjee, A Novel Approach to Noncommutativity in Planar Quantum Mechanics, *Mod. Phys. Lett. A* **17**, 631 (2002).
- [9] B. Chakraborty, S. Gangopadhyay, and A. Saha, Quantum mechanical systems interacting with different polarizations of gravitational waves in noncommutative phase space, *Phys. Rev. D* **70**, 107707 (2004).
- [10] F. G. Scholtz, B. Chakraborty, S. Gangopadhyay, and A. G. Hazra, Dual families of noncommutative quantum systems, *Phys. Rev. D* **71**, 085005 (2005).
- [11] K. Li and S. Dulat, The Aharonov-Bohm effect in noncommutative quantum mechanics, *Eur. Phys. J. C* **46**, 825 (2006).
- [12] R. V. Mendes, Some consequences of a non-commutative space-time structure, *Eur. Phys. J. C* **42**, 445 (2005).
- [13] F. S. Bemca and H. O. Girotti, The noncommutative degenerate electron gas, *J. Phys. A: Math. Gen* **38**, L539 (2005).
- [14] M. Chaichian, M. M. Sheikh-Jabbari, and A. Tureanu, Hydrogen Atom Spectrum and the Lamb Shift in Noncommutative QED, *Phys. Rev. Lett.* **86**, 2716 (2001).
- [15] N. Chair and M. M. Sheikh-Jabbari, Pair Production by a Constant External Field in Noncommutative QED, *Phys. Lett. B* **504**, 141 (2001).
- [16] Y. Liao and C. Dehne, Some phenomenological consequences of the time-ordered perturbation theory of QED on non-commutative spacetime, *Eur. Phys. J. C* **29**, 125 (2003).
- [17] T. Ohl and J. Reuter, Testing the noncommutative standard model at a future photon collider, *Phys. Rev. D* **70**, 076007 (2004).
- [18] H. Garcia-Compean, O. Obregon, and C. Ramirez, Noncommutative Quantum Cosmology, *Phys. Rev. Lett.* **88**, 161301 (2002).
- [19] S. Alexander, R. Brandenberger, and J. Magueijo, Noncommutative inflation, *Phys. Rev. D* **67**, 081301(R) (2003).
- [20] V. Parigi, A. Zavatta, M. Kim, and M. Bellini, Probing Quantum Commutation Rules by Addition and Subtraction of Single Photons to/from a Light Field, *Science* **28**, 1890 (2007).
- [21] M. S. Kim, H. Jeong, A. Zavatta, V. Parigi, and M. Bellini, Scheme for Proving the Bosonic Commutation Relation Using Single-Photon Interference, *Phys. Rev. Lett.* **101**, 260401 (2008).
- [22] A. Zavatta, V. Parigi, M. S. Kim, H. Jeong, and M. Bellini, Experimental Demonstration of the Bosonic Commutation Relation via Superpositions of Quantum Operations on Thermal Light Fields, *Phys. Rev. Lett.* **103**, 140406 (2009).
- [23] W. P. Schleich, *Quantum Optics in Phase Space* (Wiley-VCH, Berlin, 2001).
- [24] W. Vogel and D.-G. Welsch, *Quantum Optics*, 3rd ed. (Wiley-VCH, New York, 2006).
- [25] G. S. Agarwal, *Quantum Optics*, (Cambridge University Press, Cambridge, 2013).
- [26] G. Grynberg, A. Aspect, and C. Fabre, *Introduction to Quantum Optics*, (Cambridge University Press, Cambridge, 2010).
- [27] L. Knöll, W. Vogel, and D.-G. Welsch, Action of passive, lossless optical systems in quantum optics, *Phys. Rev. A* **36**, 3803 (1987).
- [28] J. D. Cresser, Intensity correlations of frequency-filtered light fields, *J. Phys. B* **20**, 4915 (1987).
- [29] L. Knöll, W. Vogel, and D.-G. Welsch, Spectral properties of light in quantum optics, *Phys. Rev. A* **42**, 503 (1990).
- [30] A. Christ, B. Brecht, W. Mauerer, and C. Silberhorn, Theory of quantum frequency conversion and type-II parametric down-conversion in the high-gain regime, *New J. Phys.* **15**, 053038 (2013).
- [31] N. Quesada and J. E. Sipe, Effects of time ordering in quantum nonlinear optics, *Phys. Rev. A* **90**, 063840 (2014).
- [32] N. Quesada and J. E. Sipe, Time-Ordering Effects in the Generation of Entangled Photons Using Nonlinear Optical Processes, *Phys. Rev. Lett.* **114**, 093903 (2015).
- [33] N. Quesada and J. E. Sipe, High efficiency in mode-selective frequency conversion, *Opt. Lett.* **41**, 364 (2016).
- [34] F. Krumm, J. Sperling, and W. Vogel, Multi-time correlation functions in nonclassical stochastic processes, *Phys. Rev. A* **93**, 063843 (2016).
- [35] W. Vogel and R. L. de Matos Filho, Nonlinear Jaynes-Cummings dynamics of a trapped ion, *Phys. Rev. A* **52**, 4214 (1995).
- [36] F. Krumm and W. Vogel, Time-dependent nonlinear Jaynes-Cummings dynamics of a trapped ion, *Phys. Rev. A* **97**, 043806 (2018).
- [37] T. Lipfert, F. Krumm, M. I. Kolobov, and W. Vogel, Quantum effects of operator time ordering in the nonlinear Jaynes-Cummings model, *arXiv:1809.04391*.
- [38] W. Nagourney, J. Sandberg, and H. Dehmelt, Shelved optical electron amplifier: Observation of quantum jumps, *Phys. Rev. Lett.* **56**, 2797 (1986).
- [39] Th. Sauter, W. Neuhauser, R. Blatt, and P. E. Toschek, Observation of Quantum Jumps, *Phys. Rev. Lett.* **57**, 1696 (1986).
- [40] J. C. Bergquist, Randall G. Hulet, Wayne M. Itano, and D. J. Wineland, Observation of Quantum Jumps in a Single Atom, *Phys. Rev. Lett.* **57**, 1699 (1986).
- [41] D. M. Meekhof, C. Monroe, B. E. King, W. M. Itano, and D. J. Wineland, Generation of Nonclassical Motional States of a Trapped Atom, *Phys. Rev. Lett.* **76**, 1796 (1996).
- [42] R. L. de Matos Filho and W. Vogel, Quantum Nondemolition Measurement of the Motional Energy of a Trapped

Atom, Phys. Rev. Lett. **76**, 4520 (1996).